Precise EWOD Top Plate Positioning Using Inverse Preisach Model Based Hysteresis Compensation

Yiyan Li and R. Jacob Baker

Department of Electrical and Computer Engineering
University of Nevada, Las Vegas
Las Vegas, NV 89154-4026, USA.
liy10@unlv.nevada.edu

***Abstract*— The displacement of an intelligent PZT (piezoelectric materials based on modified lead zirconate titanate) controlled EWOD (electrowetting on dielectric) top plate is modeled by inverse Preisach hysteresis algorithm. First, the PZT deflection model is created from an experimental displacement dataset. The real time output is predicted based on the previously stored weighting functions. Upon the desired output and the current input, the input voltage is compensated by a feedforward voltage which is derived from the model using a closest match method. The feedforward process and the model are stored in a PC. A portable high voltage DAC (digital-to-analog converter) is used to drive the PZT cantilever structure. The worst-case DNL of the high voltage DAC is 0.8125 mV. The tracking errors of a 0.067 Hz triangle wave input are less than 5 µm. Results show the inverse Preisach model is a good candidate for precise EWOD top plate displacement hysteresis compensation.**

Keywords—electrowetting; gap height; PZT; Preisach hysteresis; digital microfluidics

I. INTRODUCTION

Droplet level microfluidics has been realized by electrowetting on dielectric (EWOD) digital microfluidic (DMF) chips [1-4] and dielectrophoresis (DEP) [5]. The biggest advantage of EWOD over DEP is its capability of operating in an oil-free EWOD chamber [4] which makes EWOD stand out among all the DMF techniques for its flexibility in droplet operations. There are mainly two types of EWOD topologies. One is the single-plate topology; the other one is the dual-plate topology. The evaporation of the liquid in the single-plate system is a big problem. The droplet is in micro-liter or nano-liter level, so the evaporation during the experimental process is significant. The dual plate system is more robust and versatile because of less evaporation and the capability of operating more droplet behaviors such as dispensing, merging, actuating and splitting [6]. With a global grounded top plate, only the target electrode needs to be activated for actuation and all the other unused electrodes are floated. The single plate configuration requires the neighboring electrodes to be grounded, which leads to low usage efficiency of the electrode array. The switch-like control of the electrodes in the dual plate configuration is more interface-friendly to digital electronics. However, the gap height (top plate height) has a great influence on droplet manipulation [7] in a dual plate system and thus a height adjustable top plate is desirable. In this paper a precise top plate positioning technique is achieved by using two bimorph piezoelectric cantilever beams (PZT material). The PZT plate is capable of delivering sub-micron displacements with several millivolts of applied control voltage [8]. Because of the outstanding performance in resolution, stiffness and bandwidth, piezoelectric actuators are widely used for accurate positioning tasks [9]. Because of the displacement-to-voltage nonlinearity of the PZT plate [10], an intelligent control model is required for accurate positioning. Modeling the displacement based on history measurements can predict future displacements [11] and shorten the convergence time. There are several popular modeling techniques such as Maxwell Model [12], Jiles-Atherton model [13], Duhem model & Prandtl-Ishlinskii model [14] and Preisach model [15]. The Preisach model is the most successful method for modeling a system's magnetic hysteresis [16]. By using the hysteresis models, the physical hysteresis is partially compensated and the piezoelectric actuations are linearized versus with the input voltages.

In this study, an inverse Preisach model is developed for the PZT mounted EWOD top plate displacement tracking system. Experimental first order reversal curves are used for the model. Potential applications of the proposed model are discussed.

II. MATERIALS AND METHODS

A. System design

The top plate is mounted to two PZT plates which are fixed by two binding posts on the other end. The top plate ITO (indium tin oxide) side is grounded all the time for proper droplet operations. A high voltage module purchased from EMCO (EMCO F40, Schweiz, Switzerland) is used as the high voltage source to provide the driving voltages to the PZT chip and the EWOD electrodes. The great benefit of using EMCO driving circuit is saving the space of using bench function generators & amplifiers. A laser displacement sensor (Z4M-S40, Kyoto, Japan) and its manufactural amplifier (Z4M-W40, Kyoto, Japan) are used to monitor the PZT displacement. The laser displacement sensor can perform high resolution (100 nm), high bandwidth (1 kHz) and non-contact displacement measurement. Fast and precise displacement data can be achieved without affecting the mechanical vibration properties of the structure.

Instead of using a bench signal generator and amplifier, an MCU (PIC24fJ96, 16 bits) and a DAC (MCP4921, 12 bits,

978-1-4673-7980-9/15/$31.00 ©2015 IEEE

SPI interface) module are used to generate the high voltage triangle waves (Fig. 1b). The output voltage of Z4M-W40 is 0-200 mV, so a second stage inverting amplifier is required to levitate the voltage level for the ADC (ADC, 0-3.3 V) (Fig. 1b). To avoid op-amp saturation, the gain of the inverting op-amp is set less than 10; so another noninverting op-amp is needed as the third stage amplifier. Offset voltages for these two op-amps should be tuned with potentiometers in series with the resistors (Fig. 1b).

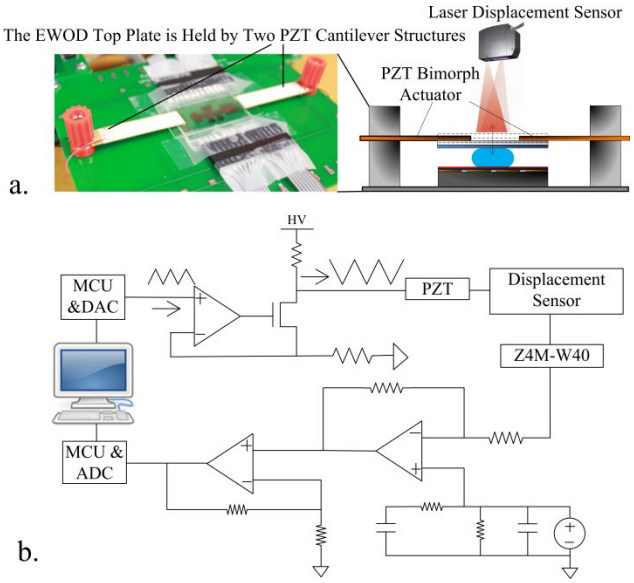

Fig. 1 (a) The experiment setup of the EWOD system and the cross section of the PZT cantilever structure with the EWOD system. (b) The proposed portable EWOD top plate positioning system.

A desktop PC (ASUS, Intel i5 2.53 GHz, RAM 8 GB) is used for data collection and sending driving voltages to the DAC & MCU module. The DAC translates the digital driving voltages to 0-2.7 V. An additional linear high voltage amplifier is developed to modulate the 0-2.7 V to 0-200 V to drive the PZT plates (Fig. 1).

B. The Preisach hysteresis model

Mathematical models for PZT can predict the displacement output and compensate for the nonlinearity. With a set of linear voltage input (reversal), the hysteresis of the PZT displacement has nonlinearity curves that are similar to an ascending exponential curve and a descending logarithmic curve. The mathematical model based on the interaction of the charges and the polarization of the internal dipoles is highly dependent on different types of PZT chips [17]. Preisach hysteresis model is independent of the physical properties of the PZT chips. The extremum of the ascending (α) and the descending (β) curves are set as the x and y limit respectively. Different (α, β) pairs can be tested. The (α, β) pairs are also called hysterons of the system. For multiple first order reversal curves, the memory curve structure for the Preisach operator is formed by different hysteron pairs. P+ and P− are the regions on the Preisach plane where the corresponding hysteron outputs are positive and negative respectively. The corners of the memory curve remember the dominant maximum and minimum values of the input in the past (Fig. 2).

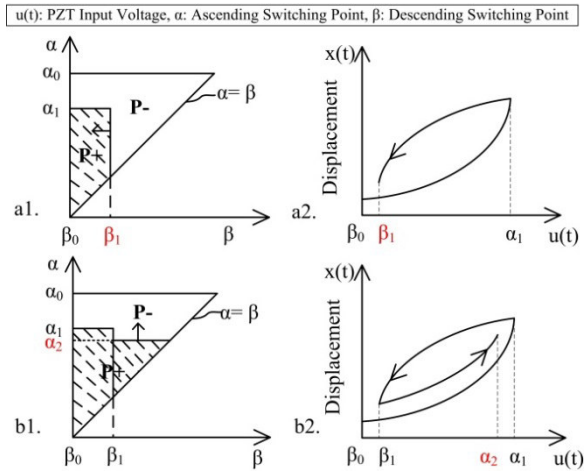

Fig. 2 The multiple first order reversal curves and their corresponding representations in the Preisach triangle.

It is obviously that when α increases, the area of the shaded parts in Fig. 2 increases exponentially; when β decreases, the shaded area decreases logarithmically. The shaded areas in the triangle model behave very similar to the displacement hysteresis of the PZT chips. With this geological model and a proper weighting value for each hysteron pair, the voltage to displacement hysteresis loops can be predicted.

The first order reversal curve in the Preisach model is used for the PZT displacement test. The experimental input voltage and the corresponding output is shown in Fig. 3a. This curve is the result of the integral of the input voltage in both ascending and descending directions. The result of the input integration is a dimensionless parameter. The actual PZT displacement curve looks similar to this curve but needs to be fitted by the curve in Fig. 3a by dividing the weighting function (Fig. 3b) for each sampled points.

The Preisach model is given as:

$$\mathrm{x(t)} = \iint_{P+} \mu(\alpha,\beta)\gamma_{\alpha\beta}[u(t)]d\alpha d\beta - \iint_{P-} \mu(\alpha,\beta)\gamma_{\alpha\beta}[u(t)]d\alpha d\beta \quad (1)$$

$$\mu(\alpha'\beta') = \frac{\partial x(\alpha',\beta')}{\partial\alpha'\partial\beta'} \quad (2)$$

where $\gamma_{\alpha\beta}[u(t)]$ is the operator which has a value of 1 or 0. $d\alpha d\beta$ defines the unit area of each hysteron pair in the Preisach triangle. $\mu(\alpha,\beta)$ is the weighting function which is a coefficient matrix to model the dynamic triangle area hysteresis curves to the real displacement hysteresis curve. In other words, the integral of the dynamic triangle areas has a similar shape with the real PZT displacement curves; the weighting function $\mu(\alpha,\beta)$ is used to project each element in the model matrix to the real displacement matrix. Since the PZT chip displacement has a good repeatability, the previous experimental data can be used to create this weighting

function matrix; so future nonlinear displacements can be predicted.

To discretize the Peisach model, Eq. 1 can be treated as a summation of the P+ and the P- triangle areas (Fig. 2). Using the double differentiation in Eq. 2 to solve the weighting function $\mu(\alpha,\beta)$ is not acceptable for the numerical computation. The weighting function matrix is obtained using a set of experimental displacement curves divided by the integration of the input voltages.

When the input is increasing monotonically, the discretized algorithm is introduced as:

$$x(\mathrm{n})_{P+} = \sum_{n=1}^{K}[(\alpha_n - \alpha_0)^2/2] \quad (3)$$

$$x(\mathrm{n})_{P-} = \sum_{n=1}^{K}[(\beta_k - \beta_n)^2/2] \quad (4)$$

where K is the number of the total input voltage values. α_n is the current ascending element, α_0 is the start ascending hysteron, β_n is the current descending sample, β_k is the start descending hysteron. The integration of the Preisach triangle area can be represented as:

$$x(\mathrm{n}) = x(\mathrm{n})_{P+} - x(\mathrm{n})_{P-}$$
$$= \sum_{n=1}^{K}[(\alpha_n - \alpha_0)^2/2] - \sum_{n=1}^{K}[(\beta_k - \beta_n)^2/2] \quad (5)$$

A typical Preisach modeling curve obtained from the experimental data is shown in Fig. 3a. The corresponding weighting function is shown in Fig. 3b. The first order reversal hysteresis loop shown in Fig. 3a has a similar shape to the real PZT hysteresis loops.

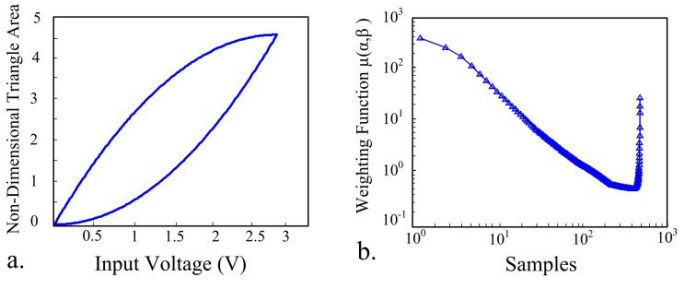

Fig. 3 (a) Integration of the linear voltage input (not real displacement). The ascending curve represents the increasing area of the Preisach triangle. The descending curve represents the decreasing area of the Preisach triangle. (b) The weighting function (coefficient matrix) used to project the obtained integration values to the predicted PZT displacement curves.

The ascending curve is below the linear curve 'x=y'; so if the desired output is 2 V, the input should be larger than 2 V. The exact value for the desired output is extracted from the model. Based on the previous experimental dataset, the corresponding input for the 2 V output can be found. If the desired voltage is not in the dataset, the closest matched data should be used as the predicted input.

For example the model is designed as $\alpha_k = \beta_k$, which means the linear model is the same as y=x, and the output range should be the same as the input range. In this case, the desired output has the same values to the input. When the input values are sampled by the ADC and integrated by the Preisach model, the software in the PC starts searching the closest output values in the previous experimental hysteresis curves and their corresponding input. Then a feedforward loop is used to compensate the initial input to linearize the output. Using the feedforward compensation, the PZT system can be treated as a linear system, and then eliminate the remaining errors using a PID (proportional-integral-derivative) or a PI (proportional-integral) controller.

III. Results and Discussions

The differential nonlinearity (DNL) of the high voltage DAC was tested, Fig. 4. The input voltage to the DAC is increased from 0 V to 2.7 V. For the 12 bit DAC, one LSB is 0.65 mV in theory. In the real test, an 11 bit DAC is used. For each 8 digits increase in the input to the DAC can cause 1 V increase at the high voltage DAC; so the real LSB is 1.3 mV and the gain of the DAC amplifier is 1 V / 8×1.3 mV = 96.15. The worst DNL is around 5/8 LSB, which is 0.8125 mV, which is good enough for our hundred-volts level applications (Fig. 4).

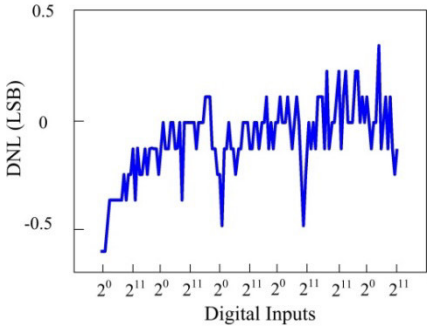

Fig. 4 The DNL of the high voltage DAC.

The first order reversal curve is shown in Fig. 5a. The input is 0-2.7 V, 0.067 Hz triangle waves. The inverse Preisach model of the hysteresis is shown in Fig. 5b. The summation of the two curves is shown in Fig. 5c, which has a very good linearity.

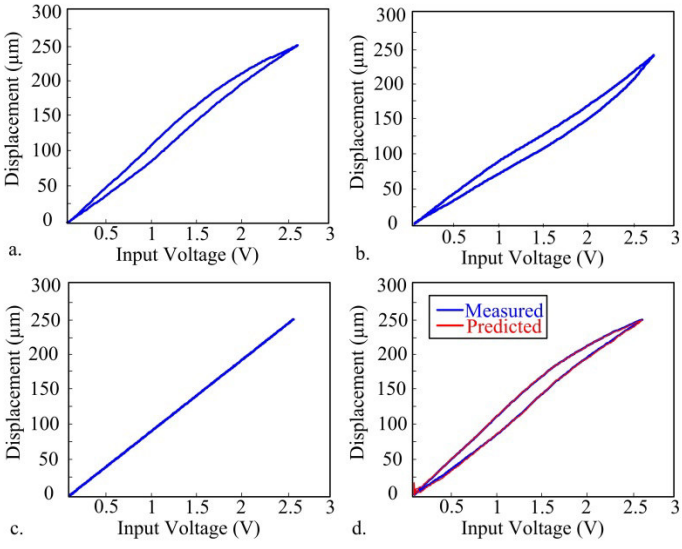

Fig. 5 (a) The experimental first order ascending and descending curves. (b) The inverse Preisach model. (c) The linearized result. (d) The measured and the predicted displacement hysteresis loop.

The first period of the triangle wave is used to build the Preisach model (Fig. 6a); the sampled four periods are tested in the tracking experiment. The largest error shown in the tracking experiment is less than 5 µm (Fig. 6b) without using any feedback controller. The most significant errors happened at small ascending hysterons (Fig. 6b). This can be improved by interpolating the modeling curves in Fig. 3a so that the phase differences of the modeled curves and the real time input voltages have less influence on the displacement.

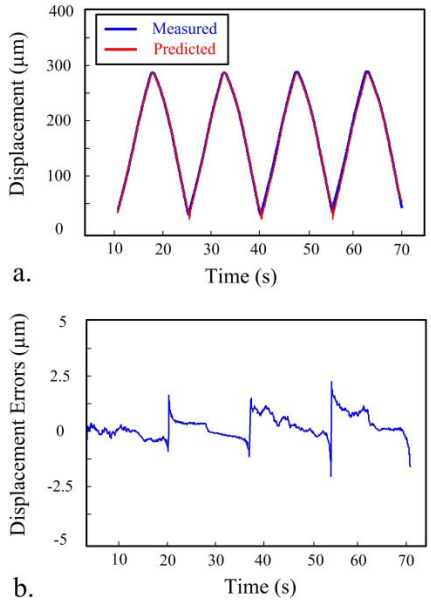

Fig. 6 (a) EWOD top plate displacement tracking. (b) Tracking errors between the real displacement and the prediction.

IV. CONCLUSION

A feedforward compensated PZT controlled EWOD top plate system is proposed in this study. The PZT cantilever structure is used to position the top plate in an EWOD system. A first order Preisach reversal curve is used to model the nonlinearity of the PZT displacements. The Preisach model is used to predict the deflection of the PZT-mounted EWOD top plate. The proposed linear high voltage DAC has a worst-case DNL of 0.8125 mV, which works well as a submicron PZT driver. The tracking error for a 0.067 Hz triangle wave input is less than 5 µm. The top plate control system is modeled in this study. Results show the inverse classic Preisach model can be used to precisely control the gap height in an EWOD system.

REFERENCE

[1] Y. Li, H. Li, R.J. Baker, A low-cost and high-resolution droplet position detector for an intelligent electrowetting on dielectric device, Journal of Laboratory Automation. 1 (2015) 1-7.

[2] Y. Li, H. Li, R.J. Baker, Volume and concentration identification by using an electrowetting on dielectric device, Proceedings of 10th IEEE Dallas Circuits and Systems Conference. (2014) 1-4.

[3] Y. Li, R. Chen, R.J. Baker, A fast fabricating electro-wetting platform to implement large droplet manipulation, Proceedings of the IEEE 57th International Midwest Symposium on Circuits and Systems. (2014) 326-329.

[4] A.H. Ng, B.B. Li, M.D. Chamberlain, A.R. Wheeler, digital microfluidic cell culture, Annu. Rev. Biomed. Eng. 17 (2015).

[5] F. Fabbri, S. Carloni, W. Zoli, P. Ulivi, G. Gallerani, P. Fici, E. Chiadini, A. Passardi, G.L. Frassineti, A. Ragazzini, Detection and recovery of circulating colon cancer cells using a dielectrophoresis-based device: KRAS mutation status in pure CTCs, Cancer Lett. (2013).

[6] S.K. Cho, H. Moon, C. Kim, Creating, transporting, cutting, and merging liquid droplets by electrowetting-based actuation for digital microfluidic circuits, Microelectromechanical Systems, Journal of. 12 (2003) 70-80.

[7] M. Yafia, H. Najjaran, High precision control of gap height for enhancing principal digital microfluidics operations, Sensors Actuators B: Chem. 186 (2013) 343-352.

[8] Y. Li, R.J. Baker, Computer vision assisted measurement of the displacements of a bimorph piezoelectric cantilever beam, IEEE Biomedical Circuits and Systems Conference (2015) 1-4.

[9] D. Walters, J. Cleveland, N. Thomson, P. Hansma, M. Wendman, G. Gurley, V. Elings, Short cantilevers for atomic force microscopy, Rev. Sci. Instrum. 67 (1996) 3583-3590.

[10] I.D. Mayergoyz, Mathematical models of hysteresis, Magnetics, IEEE Transactions on. 22 (1986) 603-608.

[11] P. Ge, M. Jouaneh, Modeling hysteresis in piezoceramic actuators, Precis Eng. 17 (1995) 211-221.

[12] M. Goldfarb, N. Celanovic, A lumped parameter electromechanical model for describing the nonlinear behavior of piezoelectric actuators, Journal of dynamic systems, measurement, and control. 119 (1997) 478-485.

[13] L.R. Dupre, R. Van Keer, J.A. Melkebeek, Identification of the relation between the material parameters in the Preisach model and in the Jiles–Atherton hysteresis model, J. Appl. Phys. 85 (1999) 4376-4378.

[14] S. Bashash, N. Jalili, Robust multiple frequency trajectory tracking control of piezoelectrically driven micro/nanopositioning systems, Control Systems Technology, IEEE Transactions on. 15 (2007) 867-878.

[15] G. Song, J. Zhao, X. Zhou, D. Abreu-García, J. Alexis, Tracking control of a piezoceramic actuator with hysteresis compensation using inverse Preisach model, Mechatronics, IEEE/ASME Transactions on. 10 (2005) 198-209.

[16] Z. Chi, M. Jia, Q. Xu, Fuzzy PID feedback control of piezoelectric actuator with feedforward compensation, Mathematical Problems in Engineering. 2014 (2014).

[17] M. Bazghaleh, S. Grainger, M. Mohammadzaheri, B. Cazzolato, T. Lu, A digital charge amplifier for hysteresis elimination in piezoelectric actuators, Smart Mater. Struct. 22 (2013) 075016.